Journal of Chromatography A, 1218 (2011) 4934–4943

Contents lists available at ScienceDirect

Journal of Chromatography A

journal homepage: www.elsevier.com/locate/chroma

Evaluation of different column types for the hydrophilic interaction chromatographic separation of iron-citrate and copper-histidine species from plants

Jessica Köster[a], Rongli Shi[b], Nicolaus von Wirén[b], Günther Weber[a,*]

[a] Leibniz-Institut für Analytische Wissenschaften – ISAS – e.V., Bunsen-Kirchhoff-Str. 11, D-44139 Dortmund, Germany
[b] Leibniz-Institut für Pflanzengenetik und Kulturpflanzenforschung, Corrensstr. 3, D-06466 Gatersleben, Germany

ARTICLE INFO

Article history:
Available online 5 April 2011

Keywords:
Metal species
Hydrophilic interaction chromatography
Iron
Copper
Plants

ABSTRACT

Hydrophilic interaction chromatography (HILIC) has emerged as a very useful separation method for polar analytes, including non-covalent metal species. Several types of stationary phases are available for HILIC applications, differing mainly in their chemical functionalities that supply additional interaction modes and alternative selectivities for the separation of special analytes. With regard to the separation of metal species only few of these stationary phases have been applied to date, and it is not completely clear what are their differences with respect to the chromatographic separation of metal species, but also with respect to species stability during chromatography. Here, a comparison of different column types for the HILIC separation of iron citrate and copper histidine species is presented and the results are discussed with respect to retention mechanisms and chromatographic stability of these metal species. It is shown that different stationary phases display very different separation patterns. In particular, three types of HILIC columns enable successful separation of iron citrates and copper histidine at pH 5.5, namely a crosslinked diol phase, a zwitterionic phase, and an amide phase. Two groups of iron-citrates are separated on all three columns, consisting of a species of 3:3 stoichiometry and another one of mainly 3:4 stoichiometry (plus 1:2 and 2:2 species). For copper-histidine only one stable species is found based on the 1:2 stoichiometry. Detection and unambiguous identification of the different species is possible by employing electrospray mass spectrometry in the negative ionization mode. Species found in standard solutions are consistent with species found in spiked plant samples. Also in unspiked solutions iron citrate of 3:4 stoichiometry (plus 1:2 and 2:2) is detectable, but no species of 3:3 stoichiometry. Significant differences of related species patterns are found in real plant samples.

1. Introduction

The transition metals iron and copper are essential micronutrients for plants. They serve as cofactors for enzymes and are required for many important physiological processes, including photosynthesis. A very complex homeostatic network exists which controls the uptake and distribution of metals in plants [1,2] but the molecular details of respective pathways are not completely known. Moreover, on many natural soils the low bioavailability of metals is a limiting factor for plant nutrition. In particular the uptake of iron is hindered, because its solubility on neutral and alkaline soils is very low. Graminaceous plants overcome this problem by secreting phytosiderophores, which are capable of mobilizing iron even from alkaline soils. This phytosiderophore-mediated uptake of iron (and other metals) is well understood [3–5] but the transport forms for long distance transport inside the plants are still under debate. One of the most promising small ligands for this task is the non-proteinogenic amino acid nicotianamine, which is structurally very similar to the phytosiderophores. Recently the role of nicotianamine as metal chelator in plants has been reviewed and an important role in transport processes of iron, copper and nickel has been highlighted [6].

The high thermodynamic stability of metal nicotianamine chelates and metal phytosiderophore chelates has promoted the development of several analytical methods for their determination. In particular, capillary electrophoresis [7,8] and hydrophilic interaction chromatography [9–11] have been applied successfully for their separation. However, even for stable species ligand exchange reactions may occur in the presence of competing ligands and/or redox mediators. For iron chelates the possibility of redox-mediated ligand exchange of the phytosiderophore 2′-deoxymugineic acid against nicotianamine [12] and direct ligand

* Corresponding author. Tel.: +49 231 1392184; fax: +49 231 1392120.
E-mail address: guenther.weber@isas.de (G. Weber).

0021-9673/$ – see front matter © 2011 Elsevier B.V. All rights reserved.
doi:10.1016/j.chroma.2011.03.036

exchange of nicotianamine against citrate [13,14] has already been demonstrated. Generally, dynamic metal–ligand systems inevitably include labile or transient metal species and special analytical methods are needed to study such labile species and their equilibria.

Iron citrate is a typical example for metal species of high biological relevance and, at the same time, low (or limited) stability. In biological studies citrate has often been one of the most promising candidates for metal chelators in plant long distance metal transport. For example, some studies showed a correlation between increased amounts of iron in plant nutrition with increasing amounts of citrate and it was possible to relate the different citrate concentrations to different nutritional states [15,16]. Studies of bacteria [17] revealed an Fe(III)-citrate transporter of the CitMHS family and in *Escherichia coli* diferric dicitrate has been shown to be involved in citrate mediated iron transport [18]. But despite all hints from biological studies very little is known about the identity of actual molecular species built from free citrate and free iron. Some theoretical calculations are available from the field of blood plasma [19] and serum analysis [20] and from analyses of sugar beet [15]. The predicted species for iron citrates are mainly of 1:1 (FeCit) and 1:2 ($FeCit_2$) stoichiometries. Structural identification of different iron citrate species was done with X-ray-spectroscopy [21]. In this study six different anionic complexes from iron and citrate were identified in crystallized form. Five of these species, with the stoichiometries 1:2, 2:2, 2:3, 3:3, and 3:4, were also identified with mass spectrometry in aqueous solution. Similar results were achieved recently [22]. It was reported that the pH and also the iron to citrate ratio plays an important role for the resulting species distribution. In spite of the identification of several iron citrate stoichiometries the work on the separation of these species in plant material just started. Rellan-Alvarez et al. [23] managed to separate at least two iron citrate species, namely a species of 2:2 stoichiometry from another one of 3:3 stoichiometry, using hydrophilic interaction chromatography on a zwitterionic (sulfobetaine type) column with MS detection.

Copper in plants is also mainly transported in complexed form. In xylem sap from chicory and tomato it was proven that at least 99.6% of copper are present as complexes [24]. Biological experiments indicate a participation of the amino acids histidin, prolin, and nicotianamin in the transport of copper inside plants and also a correlation of amino acid concentrations with respective copper concentrations [25], e.g. for histidine in *Brassica carinata* [26]. The molecular structure of copper histidine species was investigated already very early [27] and binding of copper to the aliphatic amino and carboxy groups of histidine in a 1:2 complex was proposed. Later, mass spectrometric experiments were performed to investigate different 1:1 complexes of copper and other metals with histidine [28]. Copper histidine complexes of 1:1, 1:2 and 2:2 stoichiometries were identified also by electron spin resonance spectroscopy [29].

The strong dependence of species distributions on pH and on the metal to ligand ratio is one of main concerns in the analysis of small, non-covalent metal species, such as iron citrate and copper histidine. This holds in particular for separation based methods, because an excess of free ligand is usually separated from metal species during separation (changing the metal to ligand ratio), and also the effective pH may change considerably when organic modifiers (such as methanol in RP or acetonitrile in HILIC) are used. Moreover, and unlike the situation of stable phytosiderophore or nicotianamine chelates which exist always in 1:1 stoichiometry, for iron citrate and copper histidine several stoichiometries and charge states must be considered [21,29]

In the last years hydrophilic interaction chromatography (HILIC) has been employed successfully for the separation of metal species by several research groups [9–11,23]. It enables new separation possibilities due to the fact that the HILIC partitioning mechanism (as already proposed by Alpert [30]) displays only weak, but very effective, interactions with potentially labile metal species. However, HILIC separations are done using a wide variety of column materials, resulting in a combination of the pure HILIC partitioning mechanism with additional mechanistic contributions, e.g. by anion and/or cation exchange, hydrogen-bonding, dipole interactions, etc. To date, it is not really clear which mechanistic combination(s) or column material(s) are optimal for the separation of metal species and which are not.

Hence, the main objective of this work is to investigate the influence of different column types and resulting interaction modes on the HILIC separation of small, non-covalent metal species. Iron citrate and copper histidine were chosen as analytical targets because of two reasons. First, these metal species are less stable (more labile) than the phytosiderophore and nicotianamine species, which have been successfully separated already by us and others using HILIC. Hence, these species should be more sensitive to interactions with different stationary phases, making it possible to detect small differences in chromatographic stability and separation performance due to the different materials. We are well aware, of course, that the use of relatively labile species bears the risk of species redistributions or losses during separation. However, and that is the second reason for this work, separation methods are urgently needed for the "more labile" metal species in plants, as these species are extremely important for our understanding of dynamic processes in plants involving metals.

Our results confirm that a separation of such species is possible under HILIC conditions, but considerable differences of HILIC stationary phases exist with respect to the separation of polar organic standards, and in particular with respect to the separation of metal species. Only few materials are found to be well suited for metal species analyses at the pH of the xylem (pH 5.5), including the phases with zwitterionic groups, crosslinked diol groups, and carbamoyl groups. These materials are also well suited for the analysis of small plant metabolites, including the more stable metal species, and thus open the possibility to analyze simultaneously mixtures of metal species of different stability and related ligand pools in plants.

2. Experimental

2.1. Chemicals

The amino acids histidine, aspartic acid, glutamic acid and the reduced form of glutathione were purchased from Roth (Karlsruhe, Germany) in biochemical grade (min. 98.5%). Alanine and arginine were obtained from Merck (Darmstadt, Germany) in biochemical grade (min. 99%). Phenylalanin was obtained in 99% purity (Microselect) from Fluka. Citric acid in p.a. grade was obtained from Roth (Karlsruhe, Germany) and iron nitrate in p.a. grade from Merck (Darmstadt, Germany). Ammonia was purchased as 25% aqueous solution from Fluka.

The solvents for LC–MS analysis were prepared exclusively from chemicals in LC–MS grade purity. Ammonium acetate and acetic acid were obtained from Sigma–Aldrich, acetonitrile from Carl Roth (Karlsruhe, Germany), and water from Fisher Scientific (Schwerte, Germany).

2.2. Preparation of standard solutions

Aqueous stock solutions of amino acids, glutathione, and citrate were prepared at a concentration of 10 mmol/L. The stock solutions were diluted to a concentration of 100 μmol/L in 10 mmol/L ammonium acetate, pH 5.5, containing 50% of acetonitrile. The iron citrate

Table 1
Columns used in this investigation.

	Dimensions (mm)	Particle size (μm)	Pore size (Å)	Functionality	Interaction[a] mode
Tosoh TSKgel-Amide-80	150 × 2	3	80	Carbamoyl	H-bonding
Phenomenex Luna-HILIC	150 × 2	3	200	Crosslinked diol	H-bonding
SeQuant ZIC-HILIC	150 × 2.1	3.5	200	Sulfobetaine	Weak electrostatic
Macherey-Nagel Nucleodur HILIC	125 × 2	3	110	Sulfobetaine	Weak electrostatic
Phenomenex Kinetex HILIC	100 × 2.1	2.6	100	Plain silica	Cation exch.
Phenomenex Luna NH_2	150 × 2	3.2	100	Alkylamino	Anion exch.
Tosoh TSKgel-NH_2-100	150 × 2	3	100	Alkylamino	Anion exch.
Dionex Acclaim Trinity P1	100 × 2.1	2.6	NSH[b]	SCX (surface) WAX (pores)	Cation exch. Anion exch.
Phenomenex Kinetex PFP	100 × 2.1	3	100	Pentafluoro-phenyl	Dipole–dipole H-bond, π–π
Thermo Scientific Hypersil Gold PFP	150 × 2.1	3	175	Pentafluoro-phenyl	Dipole–dipole H-bond, π–π

[a] Other than HILIC partitioning.
[b] NSH = nanopolymer silica hybrid, SCX = strong cation exchange, WAX = weak anion exchange.

standard was set up by dissolving appropriate amounts of citric acid in 10 mmol/L ammonium acetate buffer at pH 5.5. Then iron nitrate was added. The stock solution was produced at a concentration of 2 mmol/L iron and 4 mmol/L citrate. For the measurements the stock solution was diluted 1 + 1 with solvent B to yield concentrations of 1 mmol/L iron and 2 mmol/L citrate, respectively. Copper histidine standard was prepared accordingly, yielding a final concentration of 1 mmol/L copper and 5 mmol/L histidine. All dilution steps from stock solutions were prepared daily.

2.3. HILIC–MS

For all experiments with different columns the same gradient was used, consisting of acetonitrile and aqueous 10 mmol/L ammonium acetate at pH 5.5. Solvent A consisted of 90% water with 10% acetonitrile and 10 mmol/l ammonium acetate at pH 5.5. Solvent B consisted of 10% water with 90% acetonitrile and 10 mmol/l ammonium acetate at pH 5.5. The gradient started with 10% solvent A and 90% solvent B for the first 3 min. Then, a linear gradient was applied reaching a composition of 55% solvent A and 45% solvent B at 33 min. This composition was held until 45 min. Then the solvent composition was returned to the starting conditions (10% solvent A and 90% solvent B) within 5 min, and reequilibrated at that composition for at least 10 min.

ESI-MS measurements of standards were done using a LCQ Deca linear ion trap MS (Thermo Fisher Scientific, Waltham, MA, USA) in negative ionization mode, *m/z* range 120–1000. The capillary temperature was 275 °C and a spray voltage of 5 kV was applied. 5 μL of the diluted standard solutions or samples were injected after appropriate dilution into a flow of 200 μL/min by manual injection. The analytes were eluted by gradient elution. Ten different chromatographic columns were used for the experiments under HILIC conditions. The respective column types and dimensions are shown in Table 1, including their characteristic functionalities and expected interaction modes (other than HILIC partitioning).

The plant samples shown in this work are part of a larger series of plant samples, which was measured on a LTQ FT MS (Thermo Fisher Scientific, Waltham, MA, USA) in negative ionization mode. The capillary temperature was 275 °C and a spray voltage of 3.5 kV was applied. The mass range (*m/z*) was divided in three overlapping sections from 65 to 175, 150 to 500, and 475 to 1000. 20 μL of the samples were injected after appropriate dilution into a flow of 125 μL/min. The samples were separated on a 150 mm × 2.1 mm ZIC-HILIC zwitterionic column (Sequant, Umea, Sweden), particle size 3.5 μm. The gradient started with 100% solvent B for the first minute, then a linear gradient was applied reaching a composition of 75% solvent A and 25% solvent B at 25 min. This composition was held constant until 30 min, and then the solvent composition was returned to the starting conditions (100% solvent B) within 1 min and equilibrated at that composition until 45 min. This gradient is a slightly modified version of the gradient used for standards (i.e. steeper gradient but lower flow rate). The adaptation of separation and detection parameters is necessary to assure comparable results of the two LC–MS systems, and it is also advantageous for the measurement of larger series of samples. It was verified, however, that the separation and detection parameters in both systems yield essentially the same results (elution order of standards, species stability, etc.).

The data evaluation was done for both MS instruments using the Xcalibur software (Thermo Fisher Scientific, Waltham, MA, USA).

Precautions: During chromatographic separation of labile metal complexes, partial dissociation may occur resulting in metal contamination of the respective column. The relevance of this effect depends on the concentration and stability of metal species to be separated, type of sample, column and buffer. Metal contamination (especially regarding iron) affects the retention times and chromatographic resolution of analytes and may even lead to systematic errors in the analysis of metal species. We know already from previous investigations that partial dissociation of iron species may occur even for thermodynamically very stable iron phytosiderophore chelates [9]. Also for iron citrates such on-column dissociation has been observed [23]. Hence, it is essential to check periodically for such metal contamination and remove it when detected. For this purpose, we used a procedure which was already applied successfully in the analysis of phytosiderophore complexes [9]. Shortly, this procedure works by injecting free EDTA (1 mmol/L) and checking for eluting peaks other than free EDTA, namely Fe(III)-EDTA, which is easily identified by its retention time and characteristic mass spectrum (see Section 3.2.1 for details). If iron contamination is detected, it can be removed by regenerating the column with EDTA solution, followed by buffer (to remove excess EDTA), pure water (to remove any salt contamination) and finally re-equilibrating the column with the starting composition of the gradient.

2.4. Plant samples

The plant samples were prepared at the Leibniz-institute in Gatersleben as part of a study on senescence and metal remobilization. Barley plants were grown under well-controlled nutritional conditions with respect to iron deficiency, nitrogen deficiency and shading. Five biological replicates were collected for each sample type (e.g. oldest and second-oldest leaves), frozen in liquid nitrogen and ground. Afterwards each sample was extracted with doubly distilled water and centrifuged. The extracts were stored at −18 °C. Directly before analysis the samples were thawed, diluted with 50% solvent B and filtered before analysis.

3. Results and discussion

3.1. Selection and characterization of HILIC columns

In a previous investigation on the hydrophilic interaction chromatographic separation of metal species on zwitterionic stationary phases [31] we already found that the type and relative arrangement of stationary phase functionalities may have a strong influence not only on the retention of metal species, but also on their stability during chromatographic separation.

For the present investigation we initially selected 10 columns, which are listed in Table 1. All stationary phases are based on spheric silica, but differ considerably in surface functionalities and charge patterns. The Amide-80-, Diol-, and PFP columns are neutral, but support hydrogen-bonding and for the PFP-columns also dipole–dipole and π–π interactions in addition to the HILIC partitioning mechanism. Zwitterionic columns are overall neutral (balanced negative and positive charges in close vicinity) but may interact electrostatically with charged analytes. Even stronger electrostatic interaction is possible with amino-type columns (positively charged at pH 5.5) and with the Kinetex HILIC column (bare silica, negatively charged at pH 5.5). The Trinity column is a nanopolymer–silica–hybrid system, combining weak anion exchange, reversed-phase, and strong cation-exchange properties, but in contrast to the zwitterionic material the positive and negative charges are clearly spaced. This selection of columns covers a wide range of possible HILIC materials with respect to charge, polarity, and different modes of interaction.

In order to test the suitability of the selected columns for the separation of small, polar metabolites from plant material, a mixture of eight standard substances was applied to each column. These standards include two acidic amino acids (glutamic and aspartic acid), two basic amino acids (arginine and histidine), two neutral amino acids (alanine and phenylalanine), citrate, and reduced glutathione. Standards of metal species were not yet included, because their chromatographic stability and possible reactivity towards the above standards was not previously known. However, the standard mixture of small, polar molecules represents all relevant interaction modes of small metal species, i.e. electrostatic interaction, dipole interaction, hydrogen-bonding, and HILIC partitioning.

Fig. 1 depicts the chromatographic behavior of the standards on five selected columns (amide, diol, silica, and two zwitterionic materials). In general, the elution order follows the expected HILIC partitioning mechanism. In particular, phenylalanine always elutes first because of the hydrophobic phenyl moiety, the small zwitterion alanine elutes second, and the positively charged arginine is always the last eluting standard. However, the elution order of the other standards (including all negatively charged compounds and the positively charged histidine) varies considerably with the different column materials. Interestingly, the most pronounced

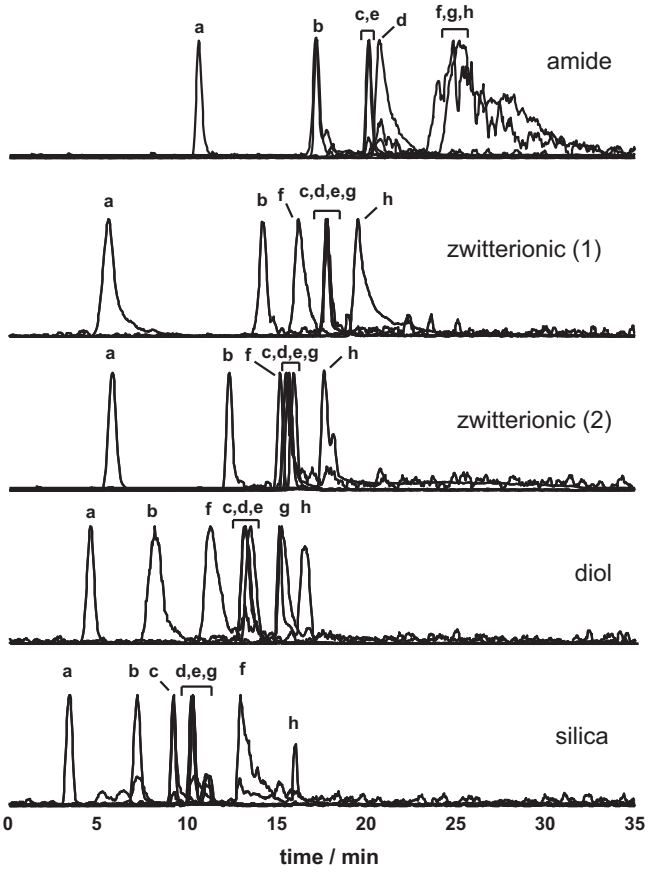

Fig. 1. Retention of standards on five HILIC columns with different functionalities. (a) Phenylalanine (*m/z* 164.1), (b) alanine (*m/z* 88.0), (c) aspartic acid (*m/z* 132.0), (d) glutamic acid (*m/z* 146.0), (e) glutathione (*m/z* 306.1), (f) histidine (*m/z* 154.1), (g) citric acid (*m/z* 191.0), (h) arginine (*m/z* 173.1). For all experiments the same gradient (ammonium acetate/acetonitrile at pH 5.5, see Section 2) was used. All peaks are normalized to the same height and are slightly smoothed (5 point boxcar averaging).

variations are observed for citrate and histidine, which will be discussed as metal-binding ligands in the next chapter. On bare silica, citrate is found in one group with the other negatively charged compounds (glutamic acid, aspartic acid, glutathione) and histidine is retained much stronger. Clearly, this is due to the interaction of the positively charged histidine with the negatively charged silanol groups. On the diol-functionalized column this electrostatic interaction is not possible and histidine elutes much earlier. At the same time citrate, which is capable of strong hydrogen-bonding interactions with the diol column via its carboxylic and hydroxy groups, is retained much stronger – resulting in a reversal of the elution order of histidine and citrate (if compared to the silica column). On the zwitterionic columns the elution order is similar to that on the diol column, but on the Amide-80 column, which is known to allow for even stronger hydrogen-bonding (compared to diol), citrate and histidine are both shifted very close to the strongly retained arginine.

Not shown in Fig. 1 are chromatographic separations on the remaining five columns (as listed in Table 1), because those columns were found not to be well suited for the separation of the standard mixture at pH 5.5. Most of the standards are hardly retained on PFP materials under HILIC conditions (exceptions are phenylalanine, histidine and arginine). Contrary to this behavior, several standards are too strongly retained on the amino-functionalized columns and also on the Trinity column. Moreover, initial experiments with metal species showed considerable dissociation of metal species on these columns, probably due to strong

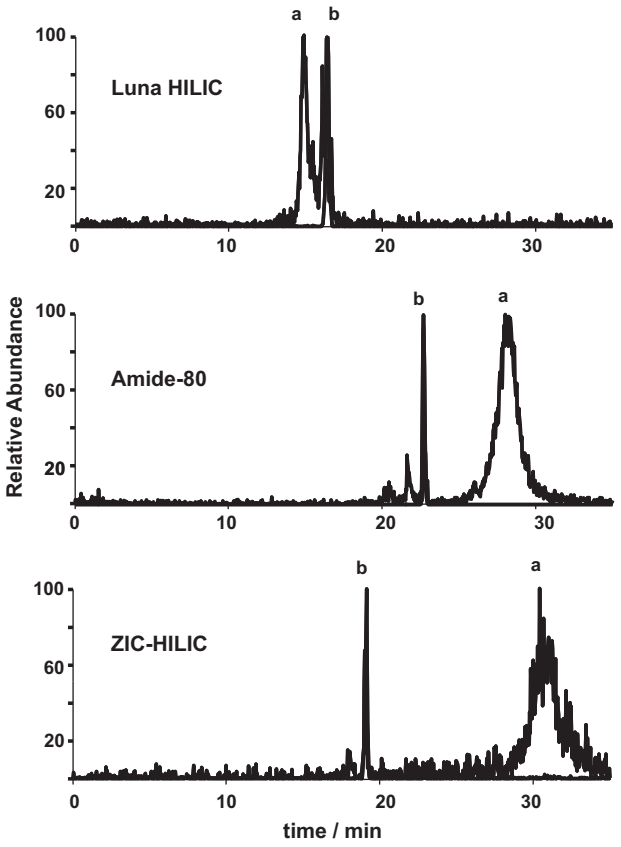

Fig. 2. Chromatographic behavior of free EDTA and its ferric complex on three HILIC columns with different functionalities. Extracted mass chromatograms are displayed at *m/z* 344.1 for ferric EDTA and at *m/z* 291.1 for free EDTA. (a) Fe(III)-EDTA and (b) free EDTA. Details of the three columns are given in Table 1.

electrostatic interactions of the species with positively charged amino-groups.

3.2. HILIC of metal species

Initially, experiments with standards of metal species were done using all 10 columns. However, as already discussed above, the PFP columns were not further investigated because of the low retention of small aliphatic compounds (including metal species) and the amino-type columns and the mixed-mode Trinity column were excluded because of too strong retention and too strong interaction with some metal species. A similar trend (too strong interaction with metal species) was also found for the bare silica column. Consequently, further experiments were restricted to three columns: the diol-, amide-, and zwitterionic (sulfobetaine) columns.

3.2.1. Chromatography of EDTA and Fe(III)-EDTA

Apart from the fact that we used EDTA as a test substance for detecting iron contamination of the columns (see Section 2), Fe(III)-EDTA is used frequently as soluble iron source in plant experiments. The chelate is bioavailable and may be taken up (at least partly) by plants from the nutrient solution, leading to varying amounts of Fe(III)-EDTA and/or the free ligand in plant compartments [7]. Hence, the chromatographic behavior of EDTA and Fe(III)-EDTA should be known if plant samples are analysed.

In Fig. 2 the chromatographic behavior of free EDTA (*m/z* 291.1) and Fe(III)-EDTA (*m/z* 344.1) on the three selected columns is shown. On the zwitterionic ZIC-HILIC column the best separation of the two substances and also the highest retention time of the ferric complex is obtained. This agrees very well with our previous investigations using the same type of column [9,31]; only the absolute retention times are slightly different due to the different gradient and pH. The respective separation on the Amide-80 column looks very similar with a higher retention of EDTA and slightly lower retention of ferric EDTA, respectively. Keeping in mind that this column bears carbamoyl functionalities, which are not charged, it is obvious that the combination of HILIC partitioning plus strong hydrogen-bonding potential (Amide-80) is as effective as the combination of HILIC partitioning plus weak electrostatic interactions (ZIC-HILIC). In contrast to this, much weaker hydrogen-bonding and no electrostatic interaction is possible on the crosslinked diol-phase (Luna HILIC), resulting in shorter retention times and a decrease of chromatographic resolution of the two peaks. Moreover, in comparison to the two other columns the elution order of EDTA and Fe(III)-EDTA is reversed on this column. This may be explained by the charge state of EDTA, which is a zwitterion at pH 5.5 (four negatively charged carboxylic groups and two protonated nitrogens [32]) with an overall charge of −2. On complexation with iron the overall charge decreases, leading to shorter retention in the classical HILIC concept (partitioning). If additional electrostatic or hydrogen-bonding interactions are allowed, however, the ferric EDTA chelate is obviously much stronger bound to the ZIC-HILIC and Amide-80 materials than the free ligand. Also the different extent of hydration may contribute to this result, but hydration numbers for EDTA and Fe(III)-EDTA were not readily available.

Table 2
Iron citrate species as detected by ESI-MS in negative ionization mode.

Species	Stoichiometry (metal/ligand)	*m/z*	Detected by MS	
			Direct infusion	After HILIC
$[(cit)H_3]^-$	0:1	191.1	y	y
$[Fe(cit)]^-$	1:1	243.9	–	–
$[Fe(cit)_2H_4]^-$	1:2	436.0	y	y
$[Fe(cit)_2H_3]^{2-}$	1:2	217.5	–	–
$[Fe_2(cit)_2H]^-$	2:2	488.9	–	–
$[Fe_2(cit)_2]^{2-}$	2:2	243.9	y	y
$[Fe_2(cit)_3H_5]^-$	2:3	680.9	y	–
$[Fe_3(cit)_3H_2]^-$	3:3	733.8	y	y
$[Fe_3(cit)_3H]^{2-}$	3:3	366.4	y	y
$[Fe_3(cit)_3(H_2O)H_2]^-$	3:3	751.8	y	–
$[Fe_3(cit)_3(H_2O)H]^{2-}$	3:3	375.9	y	y
$[Fe_3(cit)_4H_6]^-$	3:4	925.8	y	y
$[Fe_3(cit)_4H_5]^{2-}$	3:4	462.4	y	y

In the formulae, $(cit)H_4$ denotes the neutral form of citric acid.

3.2.2. Chromatography of iron-citrate(s)

In contrast to the ferric EDTA chelate, which is known to be a 1:1 hexadentate complex, the situation for iron citrate is much more complicated. As already discussed in Section 1 several Fe(III)-citrate-complexes exist, which differ in their stoichiometry and effective charge (see Table 2 for details). Even if one special pH is selected (pH 5.5 in our case) probably two, three, or even more different iron-citrates may co-exist.

In order to find out how many and which iron citrate species exist in our standard solutions (see Section 2), we used the MS instrument without chromatographic column in direct infusion mode. A typical mass spectrum in the range *m/z* 200–1000 is shown in Fig. 3. The mass spectra of all species agree with the theoretical (calculated) spectra (see supplementary material). The most intense peaks are based on an iron to citrate stoichiometry of 2:2, 3:3, and 3:4, but 1:2 and 2:3 stoichiometries are also present. The situation is complicated by the fact that from one stoichiometry several species are formed during the ionization process, for example $[Fe_3Cit_3H]^{2-}$, $[Fe_3Cit_3(H_2O)H]^{2-}$ and $[Fe_3Cit_3H_2]^-$ are readily

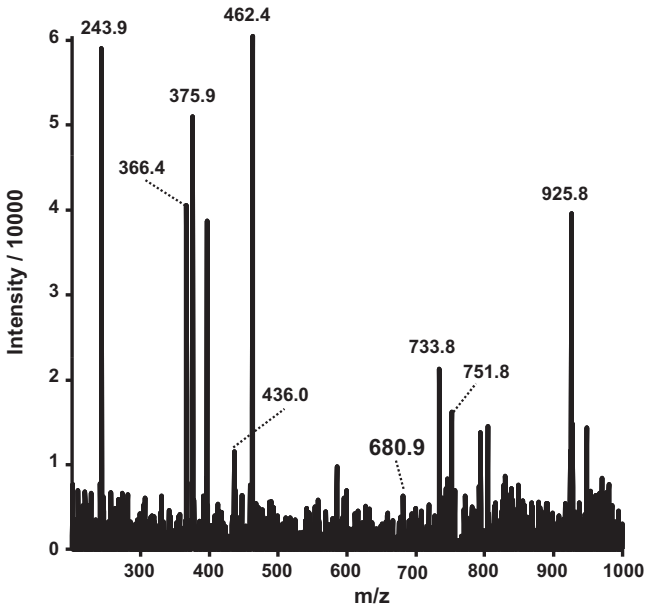

Fig. 3. Direct infusion mass spectrum of iron-citrate standard at pH 5.5. The iron to citrate ratio is 1:2, negative ionization mode was used. The formulae corresponding to the detected *m/z* values are given in Table 2.

converted into each other by protonation and hydration equilibria. Clearly, the peaks with the highest intensity are not necessarily representing the highest concentrations in solution. However, Fig. 3 illustrates well what kind of species are to be expected in real solutions at pH 5.5. It should be noted that the species distribution of Fig. 3 agrees qualitatively well with the distribution found in other experiments [21] at pH 6.5 (no data at pH 5.5 are available from this publication). In order to evaluate the influence of mass spectrometric fragmentation patterns on the species distribution, we did complementary MS/MS experiments at various collision energies. For the smaller precursor ions (1:2 and 2:2 stoichiometry) the main product ions are formed by loss of water and/or carbon dioxide, while for the bigger precursor ions (3:3 and 3:4 stoichiometry) loss of one citrate moiety was also observed. For the species of 3:4 stoichiometry a breakdown into two iron species (2:2 plus 1:2 stoichiometry) is also possible.

The chromatographic behavior of the iron citrate standard (1 mmol/L with respect to Fe plus at least twofold molar excess of citrate) is shown for the three selected columns in Fig. 4. Please note that in each case a 5 min retention time interval is shown (to display more details of the peak separation), but the absolute retention times are different, increasing in the order Luna-HILIC < Amide-80 < ZIC-HILIC. This order is similar to that already observed for ferric EDTA (see Fig. 2). In each chromatogram two separated groups of iron-citrate-species are found. The first peak group (lower retention time) always contains the iron-citrate species of 3:3 stoichiometry, while in the second peak group the species of 3:4 stoichiometry and of 1:2 and 2:2 stoichiometry are present. The retention times of the peak maxima in one group are always very similar (relative variation <1%). In spite of the very different stationary phases and related interaction modes, which result in very different retention times, the two groups of iron-citrates are always similar. Moreover, the iron-citrate-peaks are always found at higher retention times compared to the free citrate ligand (compare Fig. 1). This is again similar to the ferric EDTA system. It should be stressed that the chromatograms are well reproducible, i.e. the retention times vary by less than 2% and the variation of peak areas is in the range of 10–15% (standard deviation of triplicate injection). The iron-citrate species found after chromatography match

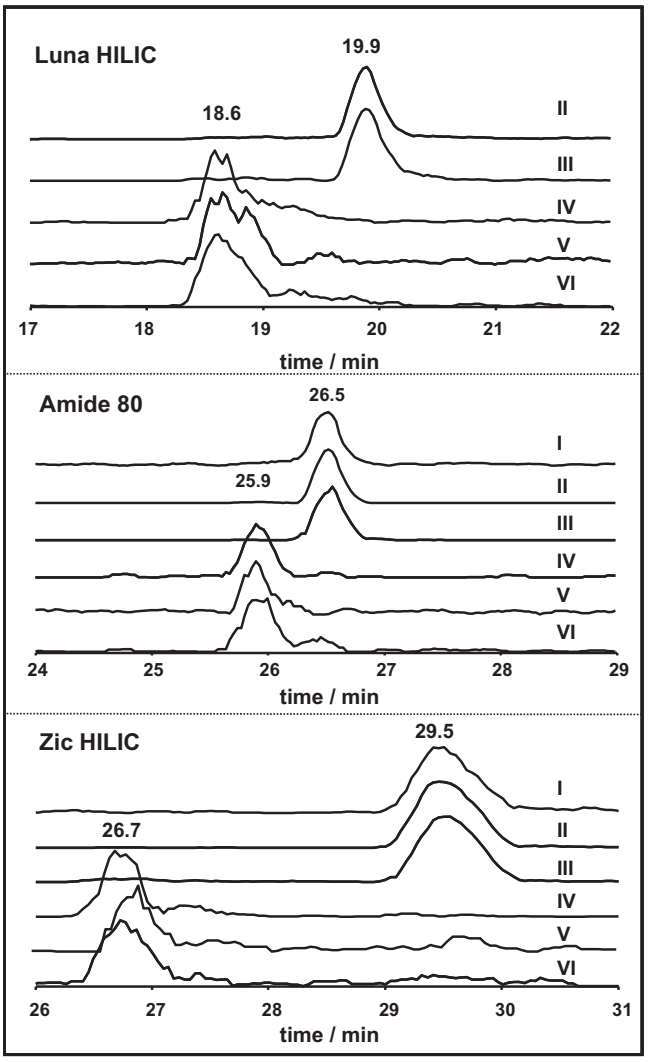

Fig. 4. Retention of iron citrate species on a diol phase (Luna HILIC), amide phase (Amide-80), and zwitterionic phase (Zic HILIC). Extracted mass chromatograms are displayed for the species I: $[Fe(cit)_2H_4]^-$ (*m/z* 436.0), II: $[Fe_3(cit)_4H_5]^{2-}$ (*m/z* 462.4), III: $[Fe_3(cit)_4H_6]^-$ (*m/z* 925.8), IV: $[Fe_3(cit)_3H]^{2-}$ (*m/z* 366.4), V: $[Fe_3(cit)_3(H_2O)H]^{2-}$ (*m/z* 375.9), VI: $[Fe_3(cit)_3H_2]^-$ (*m/z* 366.4). Chromatograms are normalized and slightly smoothed (5 point boxcar averaging).

well the respective species found in the direct infusion experiment (see Fig. 3 and Table 2), indicating that the species found after chromatography are similar to those injected.

Comparing our data with those of the only other paper available for iron-citrates in plant material [23], a relatively good agreement is found: two separate iron-citrate peaks were reported by these authors, the first one containing 3:3 stoichiometry (similar to our results), and the second containing mainly a 2:2 stoichiometry. We found mainly a 3:4 stoichiometry together with minor amounts of 1:2 and 2:2 species. Keeping in mind that the previous experiments [23] were done at elevated temperature and with methanol instead of acetonitrile, it is reasonable to find some differences. However, what seems to be different results (3:4 plus minor amounts of 1:2 and 2:2 stoichiometry (our data), versus 2:2 stoichiometry [23]) may be explained simply by different ionization/fragmentation conditions of the different MS instruments, i.e. a 3:4 species breaking down into 2:2 plus 1:2. This assumption also explains the fact that three different species are coeluting in one peak, which would seem rather unlikely if the three species are assumed to be chromatographed as separate species. In order to verify our assumption we did complementary MS/MS measure-

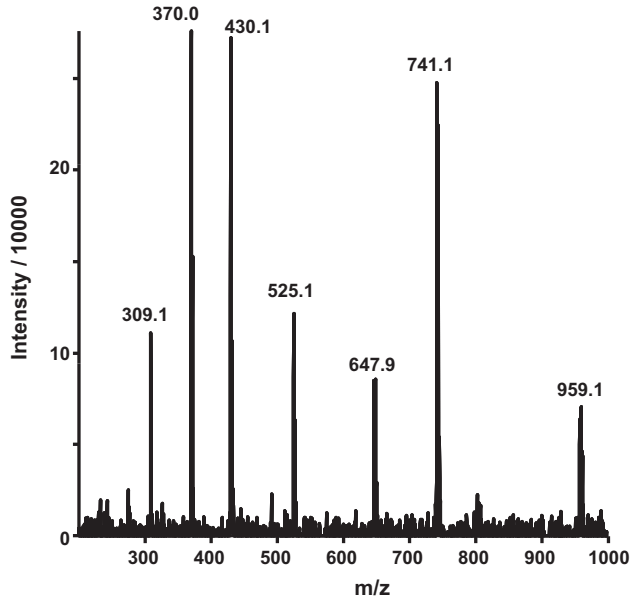

Fig. 5. Direct infusion mass spectrum of copper-histidine standard solution at pH 5.5. The copper to histidine ratio is 1:2, negative ionization mode was used. The formulae corresponding to the detected *m/z* values are given in Table 3.

ments on the fragmentation of the peak of 3:4 stoichiometry and found loss of one citrate, yielding the 3:3 species (*m/z* 733.8), as well as a breakdown into the 1:2 species (*m/z* 436.0) plus 2:2 species (*m/z* 488.9).

3.2.3. Chromatographic behavior of copper-histidine(s)

Similar to the iron-citrate system, the copper-histidine species in solution were first investigated by direct infusion MS using a solution of 1 mmol/L Cu plus 5 mmol/L histidine at pH 5.5. The respective result is depicted in Fig. 5 and the expected copper histidine species are listed in Table 3. The highest intensity is observed for the 1:2 stoichiometry (including the $[Cu(His)_2]^-$ species, the dimer $[Cu_2(His)_4]^-$, and an acetate adduct $[Cu(His)_2(Acetate)]^-$). Smaller peaks are assigned to 3:3 and 1:3 stoichiometry, and even a $[Cu_3(His)_5]^-$ species is present, which probably is an adduct of the 3:3 species and the histidine dimer. As for the iron-citrate species, the mass spectra of all species agree with the theoretical spectra (see supplementary material).

The chromatographic behavior of copper-histidine(s) and free histidine on the three selected columns is shown in Fig. 6a–c. Overall six different copper-histidine species are detectable, but only two are shown in the figure. All except the species of 1:3 stoichiometry are grouped in one chromatographic peak which is separated from free histidine. Similar to the iron-citrate and iron-EDTA systems, free histidine is eluted at shorter retention times than the copper species. Also similar to iron-citrate is the fact that the species distribution after chromatography matches well the respective distribution before chromatography (qualitatively); e.g. neither completely new species are formed during chromatography nor existing species are completely lost. The fact that all different species (except one) elute in one peak seems to indicate that only one stable Cu-histidine species exists during chromatography, which then forms different adducts and molecular forms during the ionization process. The only exception to this is the species of 1:3 stoichiometry, which on all three columns is distributed (in different ratios) between the peak of free histidine and that of the 1:2 copper-histidine peak. Actually, the 1:3 species is somehow smeared between the two peaks (at least on the Luna-HILIC and Amide-80 columns), indicating that probably a relatively labile species is formed from the main peak of 1:2 stoichiometry plus free histidine. This 1:3 stoichiometry, however, is only stable in the presence of excess of histidine and dissociates partly during chromatography, forming the stable 1:2 species plus free histidine. The fact that the chromatographic distribution of the remaining 1:3 species differs for the three columns indicates that the respective interaction modes contribute to the dissociation process. Anyway, it must be concluded that this 1:3 species is too labile for chromatographic separation (at least under the conditions tested), while the 1:2 species is stable enough. This explanation is supported also by MS/MS experiments performed on the 1:2 and 1:3 species, respectively. The 1:2 species is very stable (loosing only one or two carbon dioxide moieties with increasing energy), while the 1:3 species readily looses one histidine already at low energies, forming the stable 1:2 species as main fragment.

Table 3
Copper histidine species as detected by ESI-MS in negative ionization mode.

Species	Stoichiometry (metal/ligand)	*m/z*	Detected in MS	
			Direct infusion	After HILIC
$[(His)H_2]^-$	0:1	154.1	y	y
$[(His)_2H_5]^-$	0:2	309.1	y	–
$[Cu(His)]^-$	1:1	215.0	–	–
$[Cu(His)_2H_3]^-$	1:2	370.0	y	y
$[Cu(His)_2(HAc)H_3]^-$	1:2	430.1	y	y
$[Cu(His)_3H_6]^-$	1:3	525.1	y	y
$[Cu_2(His)_4H_6]^{2-}$	2:2	741.1	y	y
$[Cu_3(His)_3H_2]^-$	3:3	647.9	y	y
$[Cu_3(His)_5H_8]^-$	3:5	959.1	y	–

In the formulae, $(His)H_3$ denotes the neutral molecule of histidin and HAc denotes the neutral molecule of acetic acid.

3.3. Applicability of the proposed method to plant samples

The results presented so far are self-consistent and agree reasonably well with the few available literature data, but all experiments were done with standard solutions. As we wanted to develop a new method for the analysis of Fe-citrate- and Cu-histidine-species in plant material, the most important question is about the applicability of our method to real plant samples. In particular, the following questions should be answered:

(1) Does the plant matrix influence the chromatographic separation and/or the stability of metal species?
(2) Is it possible to detect iron-citrate and copper-histidine at their natural level in plant samples, and is the respective species pattern similar to that found in standards?
(3) Is it possible to distinguish biologically different plant samples with respect to the respective iron-citrate and/or copper-histidine concentrations?

In order to answer the above questions we selected some samples from an ongoing biological experiment (at the IPK Gatersleben; see Section 2.4 for details). We would like to stress that a detailed evaluation of this ongoing experiment is outside the scope of the present paper. Here, the samples are used solely as realistic plant samples, in particular with respect to metal concentrations and the presence of plant ligands.

In order to investigate the first of the above questions, we spiked one plant sample (aqueous extract of barley leaves) with our iron-citrate standard and measured the species distribution after chromatography. Fig. 7 shows the result obtained on the Amide-80 column. Only species of 3:3 stoichiometry elute in the first peak, while species of 3:4 and 1:2 (plus minor amounts of 2:2, not shown

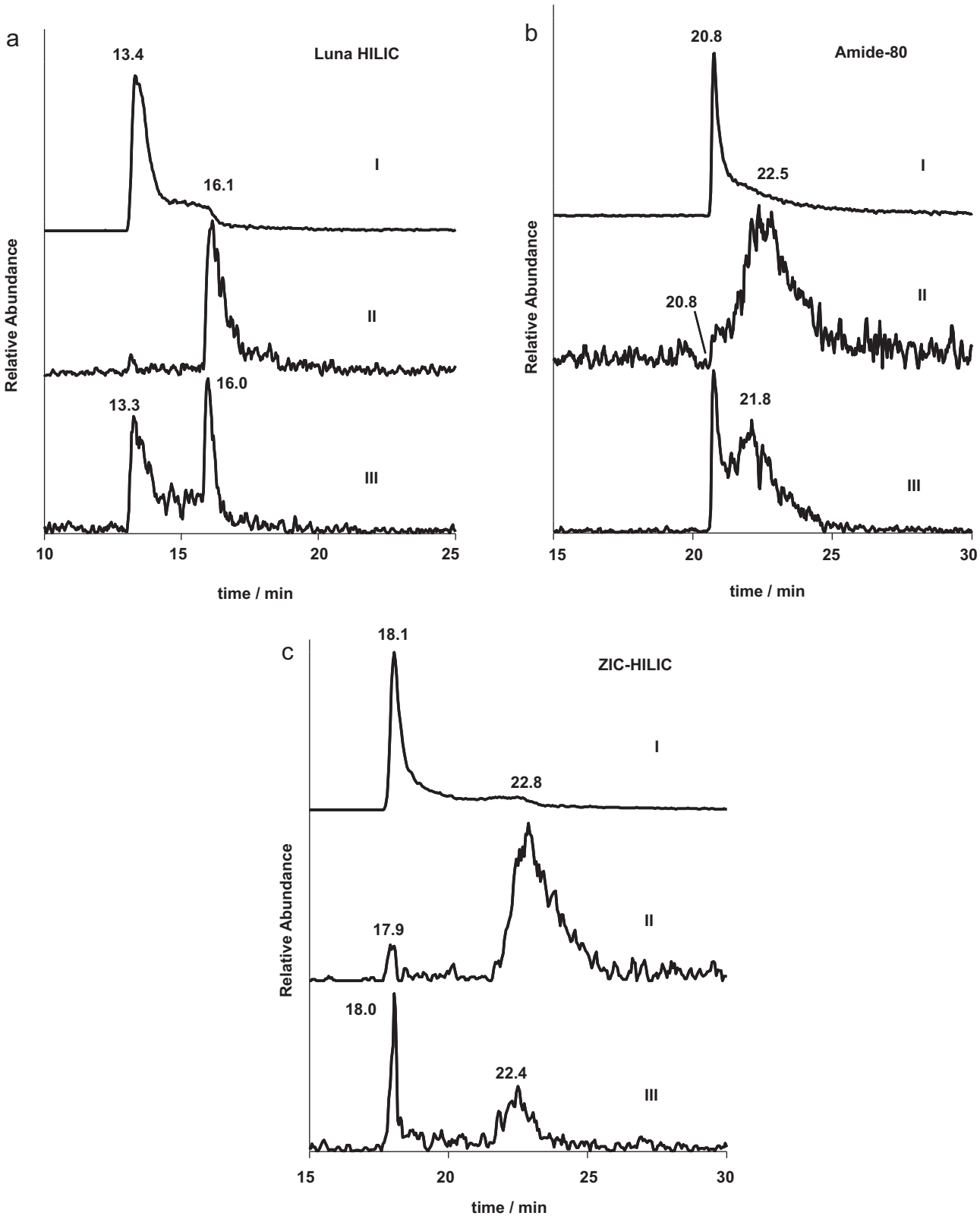

Fig. 6. Separation of copper histidine species on (a) diol phase (Luna HILIC), (b) amide phase (Amide-80), and (c) zwitterionic phase (Zic HILIC). Extracted mass chromatograms are displayed for the species I: $[His]^-$ (*m/z* 154.1), II: $[Cu\ (His)_2]^-$ (*m/z* 370.0), III: $[Cu\ (His)_3]^-$ (*m/z* 525.1). Chromatograms are normalized (largest peak = 100%).

in the figure) elute in the second peak. This species pattern of iron-citrates is very similar to that found in iron-citrate standards without plant matrix (see Fig. 4 for comparison), indicating that the plant matrix which is present in much higher concentration than the metal species does not change the chromatographic behavior of the iron citrate species.

For an analysis of unspiked plant samples we used a ZIC-HILIC column coupled to a high-resolution FTICR-MS instrument (see

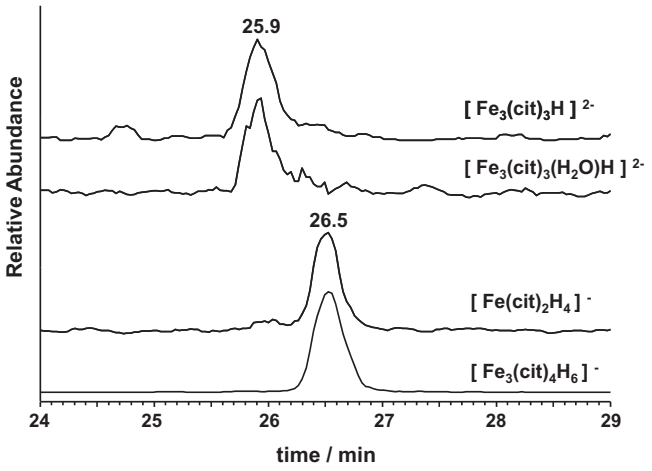

Fig. 7. Retention of iron citrate species in an extract of barley leaves spiked with iron-citrate standard. Separation was performed on the Amide-80 column, detection was done by ESI-MS in negative ionization mode. Displayed are the extracted mass chromatograms of the species $[Fe_3(cit)_3H]^{2-}$ (*m/z* 366.4), $[Fe_3(cit)_3(H_2O)H]^{2-}$ (*m/z* 375.9), $[Fe(cit)_2H_4]^-$ (*m/z* 436.0), and $[Fe_3(cit)_4H_6]^-$ (*m/z* 925.8). Chromatograms are normalized (largest peak = 100%).

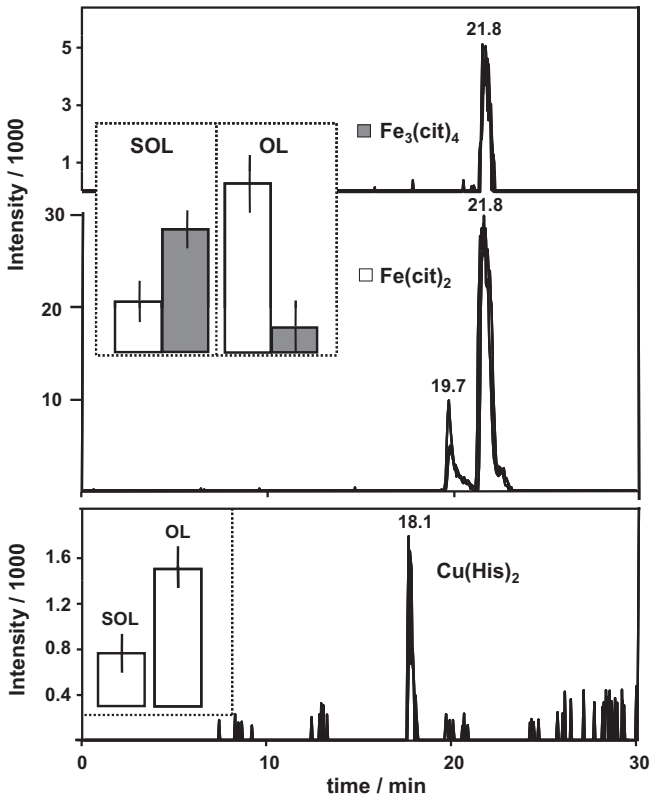

Fig. 8. Detection of iron citrate and copper histidine species in aqueous extracts of barley leaves using HILIC coupled to a high-resolution FT-ICR/MS. Extracted mass chromatograms (overlays of two replicates) are shown of the species $[Cu(His)_2]^-$ (*m/z* 370.0455), $[Fe_3(cit)_4H_6]^-$ (*m/z* 925.8351), and $[Fe(cit)_2H_4]^-$ (*m/z* 435.9582). The two insets show a comparison of copper histidine and the two iron citrate species, respectively, in oldest (OL) and second oldest (SOL) leaves. Separation was performed on a zwitterionic (Zic HILIC) column.

Section 2), because of the better sensitivity and also better mass accuracy of this instrument, which is necessary for an unambiguous identification of metal species at low concentration in complex plant samples. The total concentration of iron and copper in the plants is in the range of 10–100 mg/kg each, but the concentrations in the aqueous extracts are usually 1–2 orders of magnitude lower. Moreover, the iron citrate and copper histidine species are certainly not the only extractable iron and copper species, so the real concentration of the species is even lower. Fig. 8 demonstrates that measurements in this range are possible for iron citrate species of 3:4 and 1:2 stoichiometry and also for copper histidine species of 1:2 stoichiometry. In each case an overlay of two chromatograms (originating from two separate plant samples) is shown, demonstrating very good agreement of the data with respect to retention time, peak area and peak height. The absolute retention times differ from those of the standard measurements because of the different gradient conditions (see Section 2). Apart from that, the main difference with respect to iron citrate species found in standard solutions is the absence of any species of 3:3 stoichiometry (first peak of Fig. 4). The species of 3:4 stoichiometry are again found in one peak together with those of 1:2 and 2:2 stoichiometry (the latter is not shown in the figure but also detected). In spite of this coelution the two iron citrate species (3:4 and 1:2) can be evaluated separately due to their different mass spectra and, interestingly, a significant change of their relative amounts is found depending on the biological sample type, namely second oldest leaves (SOL) versus oldest leaves (OL); the error bars in the inset of Fig. 8 represent the standard deviation of five biological replicates. A significant difference in dependence on the sample type is also seen for the copper histidine (1:2) species, which is the only detectable copper histidine species in plant samples. The reason for this dependence of species distributions on the biological sample type is not yet clear, but analytical artifacts can be excluded (such as column contamination and memory effects). Consequently, a complete evaluation of the underlying biological experiments is presently going on based on our proposed method. This evaluation must include the citrate and histidine complexes discussed here, but also the more stable metal species (e.g. of nicotianamine and phytosiderophores, if present) and also other plant metabolites and free ligand pools.

4. Conclusions

It could be shown that different HILIC columns display very different separation patterns (and separation mechanisms) with respect to the separation of metal species. In particular three columns enabled successful separations of iron-citrates and copper-histidine at pH 5.5, namely the Luna-HILIC (crosslinked diol-phase), the ZIC-HILIC (zwitterionic sulfobetaine phase), and the TSKgel-Amide80 (carbamoyl functionalities).

Two groups of iron-citrates are separated on all three columns, consisting of a species of 3:3 stoichiometry and another one of mainly 3:4 stoichiometry, which could be interpreted probably also as an adduct of 1:2 and 2:2 species. For copper-histidine only one stable group of species was found based on the 1:2 stoichiometry, which is separated from free ligand. Detection and unambiguous identification of the different species (including different stoichiometries) is possible by employing electrospray-MS in the negative ionization mode. Species found in standard solutions are consistent with species found in spiked plant samples. For the analysis of unspiked samples, i.e. at much lower concentrations, a mass spectrometer of high sensitivity and high resolution is needed. This enabled the detection of iron citrates of 3:4 stoichiometry (plus 1:2 and 2:2), but no species of 3:3 stoichiometry were detectable. Furthermore, significant biological differences of species patterns, including iron citrates and copper histidine species, are found in real samples.

Acknowledgements

Financial support from the Deutsche Forschungsgemeinschaft (DFG, Grants WE 2422/6-2 and WI 1728/6-3), from the Ministerium für Innovation, Wissenschaft, Forschung und Technologie des Landes Nordrhein-Westfalen, and from the Bundesministerium für Bildung und Forschung is gratefully acknowledged.

Appendix A. Supplementary data

Supplementary data associated with this article can be found, in the online version, at doi:10.1016/j.chroma.2011.03.036.

References

[1] S. Clemens, Planta 212 (2001) 475.
[2] M. Pilon, C.M. Cohu, K. Ravet, S.E. Abdel-Ghany, F. Gaymard, Curr. Opin. Plant Biol. 12 (2009) 347.
[3] J.F. Briat, C. Curie, F. Gaymard, Curr. Opin. Plant Biol. 10 (2007) 276.
[4] J. Morrissey, M.L. Guerinot, Chem. Rev. 109 (2009) 4553.
[5] N. von Wirén, H. Khodr, R.C. Hider, Plant Physiol. 124 (2000) 1149.
[6] C. Curie, G. Cassin, D. Couch, F. Divol, K. Higuchi, M.L. Jean, J. Misson, A. Schikora, P. Czernic, S. Mari, Ann. Bot. 103 (2009) 1.
[7] Y. Xuan, E.B. Scheuermann, A.R. Meda, P. Jacob, N. von Wirén, G. Weber, Electrophoresis 28 (2007) 3507.
[8] M. Dell'mour, G. Koellensperger, J.P. Quirino, P.R. Haddad, C. Stanetty, E. Oburger, M. Puschenreiter, S. Hann, Electrophoresis 31 (2010) 1201.
[9] Y. Xuan, E.B. Scheuermann, A.R. Meda, H. Hayen, N. von Wirén, G. Weber, J. Chromatogr. A 1136 (2006) 73.
[10] E. Bakkaus, R.N. Collins, J.L. Morel, B. Gouget, J. Chromatogr. A 1129 (2006) 208.
[11] L. Ouerdane, S. Mari, P. Czernic, M. Lebrun, R. Lobinski, J. Anal. At. Spectrom. 21 (2006) 676.
[12] G. Weber, N. von Wirén, H. Hayen, BioMetals 21 (2008) 503.
[13] N. von Wirén, S. Klair, S. Bansal, J.F. Briat, H. Khodr, T. Shioiri, R.A. Leigh, R.C. Hider, Plant Physiol. 119 (1999) 1107.
[14] R. Rellan-Alvarez, J. Abadia, A. Alvarez-Fernandez, Rapid Commun. Mass Spectrom. 22 (2008) 1553.
[15] A.F. Lopez-Millan, F. Morales, A. Abadia, J. Abadia, Plant Physiol. 124 (2000) 873.
[16] A.F. Lopez-Millan, F. Morales, A. Abadia, J. Abadia, J. Exp. Bot. 52 (2001) 1489.
[17] J.J. Lensbouer, A. Patel, J.P. Sirianni, R.P. Doyle, J. Bacteriol. 190 (2008) 5616.
[18] V. Braun, S. Mahren, A. Sauter, BioMetals 18 (2005) 507.
[19] L.C. Konigsberger, E. Konigsberger, P.M. May, G.T. Hefter, J. Inorg. Biochem. 78 (2000) 175.
[20] R.W. Evans, R. Rafique, A. Zarea, C. Rapisarda, R. Cammack, P.J. Evans, J.B. Porter, R.C. Hider, J. Biol. Inorg. Chem. 13 (2008) 57.
[21] I. Gautier-Luneau, C. Merle, D. Phanon, C. Lebrun, F. Biaso, G. Serratrice, J.L. Pierre, Chem. Eur. J. 11 (2005) 2207.
[22] A.M.N. Silva, X. Kong, M.C. Parkin, R. Cammack, R.C. Hider, Dalton Trans. (2009) 8616.
[23] R. Rellan-Alvarez, J. Giner-Martinez-Sierra, J. Orduna, I. Orera, J.A. Rodriguez-Castrillon, J.I. Garcia-Alonso, J. Abadia, A. Alvarez-Fernandez, Plant Cell Physiol. 51 (2009) 91.
[24] M.T. Liao, M.J. Hedley, D.J. Woolley, R.R. Brooks, M.A. Nichols, Plant Soil 223 (2000) 243.
[25] M.T. Liao, M.J. Hedley, D.J. Woolley, R.R. Brooks, M.A. Nichols, Plant Soil 221 (2000) 135.
[26] B. Irtelli, W.A. Petrucci, F. Navari-Izzo, J. Exp. Bot. 60 (2009) 269.
[27] B. Sarkar, Y. Wigfield, J. Biol. Chem. 242 (1967) 5572.
[28] H. Lavanant, E. Hecquet, Y. Hoppilliard, Int. J. Mass Spectrom. 187 (1999) 11.
[29] T. Szabo-Planka, A. Rockenbauer, L. Korecz, D. Nagy, Polyhedron 19 (2000) 1123.
[30] A.J. Alpert, J. Chromatogr. 499 (1990) 177.
[31] G. Weber, N. von Wirén, H. Hayen, J. Sep. Sci. 31 (2008) 1615.
[32] Y.V. Griko, Biophys. Chem. 79 (1999) 117.